JOURNAL OF Materials CHEMISTRY

1,1′-Disubstituted ferrocene containing hexacatenar thermotropic liquid crystals†

Jin-Sung Seo, Yong-Sik Yoo and Moon-Gun Choi*

Department of Chemistry and Molecular Structure Laboratory, Yonsei University, 134 Shinchon-dong, Sodaemoon-ku, Seoul 120-749, Korea. E-mail: choim@yonsei.ac.kr

Received 7th November 2000, Accepted 20th February 2001
First published as an Advance Article on the web 23rd March 2001

The preparation and characterization of ferrocene containing hexacatenar metallomesogens **4a**–**h** based on alkoxy terminal groups with hexyloxy (**4a**), octyloxy (**4b**), decyloxy (**4c**), dodecyloxy (**4d**), tetradecyloxy (**4e**), hexadecyloxy (**4f**), octadecyloxy (**4g**) and eicosyloxy (**4h**) chains are described. The introduction of alkyl chains of different lengths induces a rich variety of self-assembled liquid crystalline structures. In the crystalline state, the ferrocene containing hexacatenar metallomesogens **4a**–**h** organize into a microphase-separated monolayer lamellar structure. In contrast, a dramatic phase change after crystalline melting of the metallomesogens is observed with variation of the chain length. The ferrocene containing hexacatenar metallomesogens **4b** and **c** display a bicontinuous cubic mesophase with *Ia3d* symmetry, while the ferrocene containing hexacatenar metallomesogens **4d**–**g** exhibit a hexagonal columnar mesophase. Further increasing the length of the alkyl chain as in the case of **4h** suppresses liquid crystallinity and induces only a crystalline phase. This unique behavior in the ferrocene containing metallomesogenic molecules can be understood to originate from the anisotropic aggregation of ferrocene containing aromatic segments and consequent entropic penalties associated with chain stretching.

Introduction

Self-organizing materials which include liquid crystalline molecules, block copolymers, hydrogen bonded complexes, and many biological polymers have been widely studied and observed to have great potential for various functional materials.[1] Manipulation of supramolecular nanostructure in self-organizing materials is of critical importance to achieving the desired functions and properties in solid state and liquid crystalline state molecular materials.[1–3] Thus, diverse molecular architectures are being explored as a means to manipulate the supramolecular structure which has dramatic effects on the physical properties of molecules. A typical example of self-assembling systems is provided by metallomesogenic molecules consisting of organic ligands and transition metals.[4] Metallomesogenic molecules containing transition metals which share certain general characteristics of both organic molecules and the metals provide typical examples for liquid crystals with high intermolecular interactions. Linear and square planar coordinations of metal atoms into conventional organic mesogens have been used to increase the aspect ratio of the aromatic core and therefore to enhance the thermal stability of both crystal and liquid crystal phases.

A large and predominant class of metallomesogens is ferrocene containing metallomesogens, ferrocene being a sandwich compound consisting of two cyclopentadienyl rings and one iron atom as center.[5–13] Ferrocene containing metallomesogens offer high thermal stability and low oxidation–reduction potential. Since the ferrocene moiety is bulky and has a more or less bent molecular structure, this offers multiple possibilities for fine tuning of the mesomorphic properties through connecting rod-like mesogenic units.

The goal of this article is to describe the synthesis and characterization of hexa-substituted rod-like metallomesogens derived from ferrocene-1,1′-dicarbonyl dichloride. We also describe the mesomorphic phase behavior of the resulting metallomesogens, characterized by a combination of DSC, optical polarized microscopy and powder X-ray scattering experiments.

Experimental

Materials

Pyridine was distilled from Na–benzophenone, CH_2Cl_2 and triethylamine from CaH_2. The solvents were stored over 4 Å molecular sieve under N_2. Ferrocene-1,1′-dicarbonyl dichloride was prepared following the literature procedure.[14] All reactions were carried out under nitrogen. Propyl 4-hydroxybenzoate (99%) propyl gallate (97%), 1,3-diisopropylcarbodiimide (DIPC, 99%), 4-(dimethylamino)pyridine (99%), 4,4′-biphenyldiol (97%), 1-bromohexane (98%), 1-bromooctane (99%), 1-bromodecane (98%), 1-bromododecane (97%), 1-bromotetradecane (97%), 1-bromohexadecane (97%), 1-bromooctadecane (96%), 1-bromoeicosane (98%), 1-bromodocosane (96%) (all from Aldrich), ferrocene (99%) (from Strem chemicals) and the other conventional reagents were used as recieved.

Techniques

^{1}H-NMR spectra were recorded from $CDCl_3$ solution on a Bruker DPX-250 spectrometer. TMS was used as internal standard. A Perkin Elmer DSC-7 differential scanning calorimeter, equipped with a 1020 thermal analysis controller

†Electronic supplementary information (ESI) available: ^{1}H NMR data of compounds **2b**–**h** and **3b**–**h**, a DSC diagram exhibited during the first heating scan by ferrocene containing hexacatenar metallomesogens, and the X-ray pattern of **4a** in a crystalline phase. See http://www.rsc.org/suppdata/jm/b0/b008904o/

 DOI: 10.1039/b008904o

was used to determine the thermal transitions which were reported as maxima of their endothermic or exothermic peaks, respectively. In all cases, heating and cooling rate were 10 °C min^{-1} unless otherwise specified. A Nikon Optiphot 2-pol optical polarized microscope (magnification:100×) equipped with a Mettler FP 82 hot stage and a Mettler FP90 central processor was used to observe the thermal transitions and to analyze the anisotropic textures. Microanalyses were performed with a Perkin Elmer 240 elemental analyzer at the Korea Research Institute of Chemical Technology. X-Ray scattering measurements were performed in transition mode with synchrotron radiation at the 3C2 X-ray beam line at Pohang Accelerator Laboratory, Korea. In order to investigate structural changes on heating, the samples were held in an aluminium sample holder which was sealed with a window of 8 mm thick Kapton films on both sides. The samples were heated with two cartridge heaters and the temperature of the samples was monitored by a thermocouple placed close to the sample. Background scattering correction was made using the scatterings from the Kapton. The correction for the slit length smearing was applied by means of Strobl's algorithm.

Synthesis

A general outline of the synthetic procedures is shown in Scheme 1.

3,4,5-Trialkoxybenzoic acid (1a–1h). **1a**–**1h** were synthesized according to the procedure reported in a previous publication.[15]

4′-Hydroxybiphenyl 3,4,5-tris(hexyloxy)phenylbenzoate (2a). Compound **1a** (3 g, 7.1 mmol), 4,4′-biphenyldiol (6.6 g, 35.5 mmol) and 4-dimethylaminopyridine (DMAP, 1.3 g, 10.7 mmol) were dissolved in 30 ml of methylene chloride and 5 ml of pyridine under nitrogen. 1,3-Diisopropylcarbodiimide (DIPC, 2.1 ml, 10.7 mmol) was added dropwise to the mixture. The mixture was stirred at room temperature under nitrogen overnight and neutralized in 1 M HCl. The resulting solution was poured into water and extracted with methylene chloride. The methylene chloride layer was washed with water, dried over anhydrous magnesium sulfate and filtered. The solvent was removed under reduced pressure and the crude product was purified by flash column chromatography (silica gel, 40–60 μm, using methylene chloride as the eluent) to yield 1.9 g (yield: 46%) of a white solid. ^{1}H-NMR ($CDCl_3$, TMS, δ, ppm): 0.85–0.88 (m, 9H, CH_3), 1.33–1.56 (m, 18H, $CH_3(CH_2)_3$), 1.74–1.86 (m, 6H, OCH_2CH_2), 4.03–4.09 (m, 6H, OCH_2), 4.93 (s, 1H, OH), 6.90 (d, 2Ar-H, *m* to OH, $J=8.6$ Hz), 7.22 (d, 2Ar-H, *m* to O_2C, $J=8.6$ Hz), 7.42 (s, 2Ar-H, *o* to CO_2), 7.47 (d, 2Ar-H, *o* to OH, $J=8.6$ Hz), 7.58 (d, 2Ar-H, *o* to O_2C, $J=8.6$ Hz).

Compounds **2b**–**2h** were prepared by a similar method to that described for compound **2a**. Their ^{1}H NMR data are available as Electronic Supplementary Information.†

4-Benzyloxybenzoic acid. 4-Hydroxybenzoic acid *n*-propyl ester (1 g, 5.5 mmol), K_2CO_3 (2.8 g, 20.6 mmol) were dissolved in 100 ml of dry THF under nitrogen. Benzyl bromide (3.5 g, 20.6 mmol) was then added to the mixture. The mixture was heated at reflux for 18 h and then cooled to room temperature. The solvent was removed under reduced pressure and excess KOH aqueous solution added. The mixture was dissolved in 100 ml of ethanol. The mixture solution was stirred at room temperature for 12 h and neutralized with HCl. The resulting solution was poured into water and extracted with methylene chloride. The methylene chloride layer was washed with water, dried over anhydrous magnesium sulfate, and filtered. The solvent was removed on a rotary evaporator to yield 1.1 g

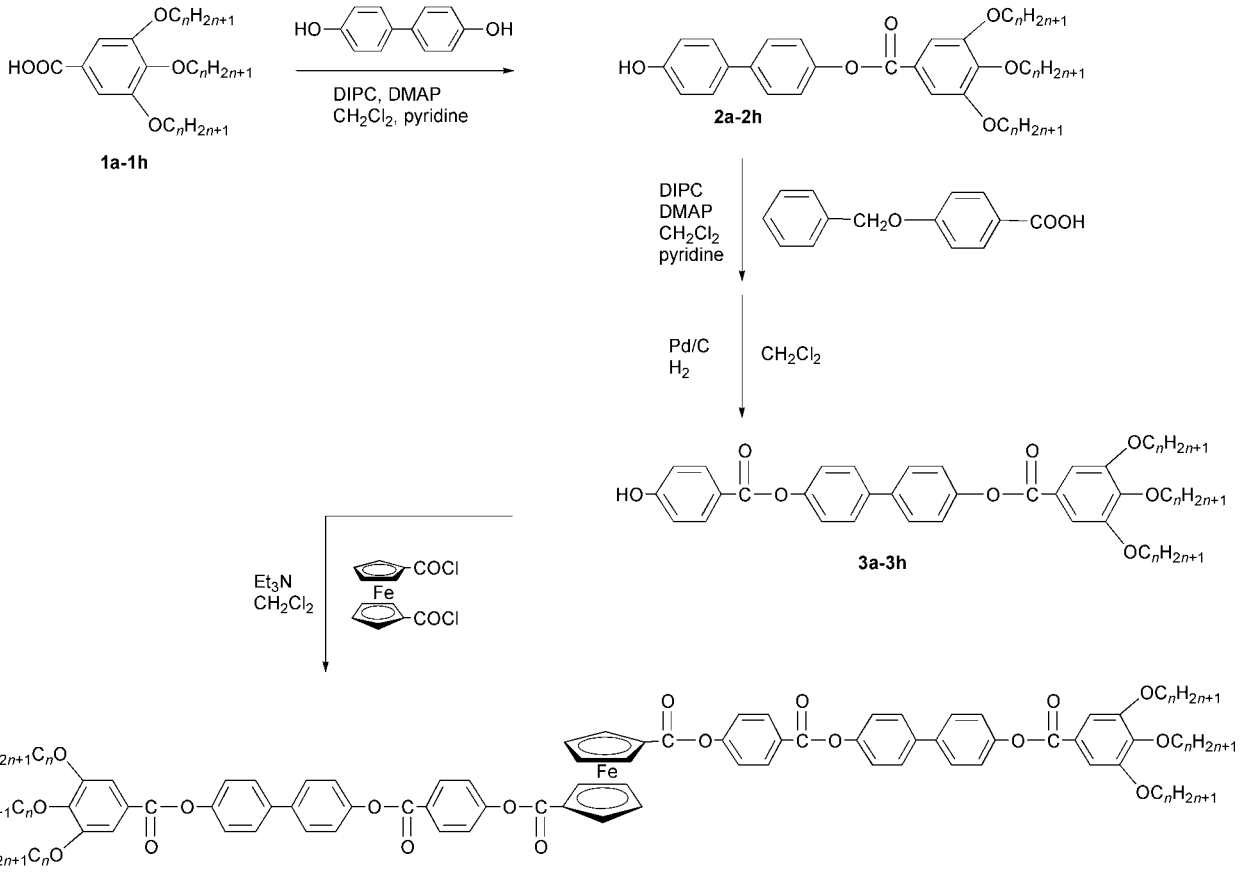

Scheme 1 Synthesis of the ferrocene containing hexacatenar metallomesogens.

(84%) of a white solid. ^{1}H-NMR ($CDCl_3$, TMS, δ, ppm): 5.14 (s, 2H, CH_2O), 7.04 (d, 2Ar-H, *m* to COOH, $J=8.8$ Hz), 7.34–7.45 (m, 5Ar-H, *Ph*-CH_2O), 8.09 (d, 2Ar-H, *o* to COOH, $J=8.8$ Hz).

4′-(4″-Hydroxyphenylcarbonyloxy)biphenyl 3,4,5-tris(hexyloxy)benzoate (3a). Compound **2a** (1 g, 1.7 mmol), 4-benzyloxybenzoic acid (0.58 g, 2.5 mmol) and 4-dimethylaminopyridine (0.30 ml, 2.5 mmol) were dissolved in 30 ml of dry methylene chloride under nitrogen, then 1,3-diisopropylcarbodiimide (0.50 ml, 2.5 mmol) was added dropwise to the mixture. The mixture was stirred at room temperature under nitrogen overnight. The resulting solution was poured into water and extracted with methylene chloride. The methylene chloride solution was washed with water, dried over anhydrous magnesium sulfate, and filtered. The solvent was removed under reduced pressure and the crude compound was isolated by flash column chromatograpy (silica gel, 40–60 μm, using methylene chloride as the eluent) to yield a white solid. The solid was dissolved in methylene chloride (80 ml) and methanol (20 ml) and then 5% palladium-on-charcoal catalyst (30 mg) was added. The mixture was stirred under a hydrogen atmosphere until no further hydrogen was taken up. Solvents were removed under reduced pressure and the residue was dissolved in methylene chloride. The catalyst was removed by filtration through Celite and the solvent was removed by evaporation under reduced pressure. After recrystallization from ethanol a white solid was obtained (0.95 g, yield: 76%). ^{1}H-NMR ($CDCl_3$, TMS, δ, ppm): 0.91–0.94 (m, 9H, CH_3), 1.25–1.56 (m, 18H, CH_3(CH_2)$_3$), 1.72–1.90 (m, 6H, OCH_2CH_2), 4.04–4.11 (m, 6H, OCH_2), 6.1 (s, 1H, O*H*), 6.82 (d, 2Ar-H, *o* to OH, $J=8.6$ Hz), 7.29 (m, 4Ar-H, 2 *m* to O_2C), 7.44 (s, 2Ar-H, tris(hexyloxy)phenyl), 7.60–7.64 (m, 4Ar-H, 2*o* (biphenyl) to CO_2), 8.07 (d, 2Ar-H, *m* to OH, $J=8.6$ Hz).

Compounds **3b**–**3h** were prepared by a similar method to that described for compound **3a**. Their ^{1}H NMR data are available as Electronic Supplementary Information.†

Bis{4-[4′-(3″,4″,5″-tris(hexyloxy)phenylcarbonyloxy)biphenyloxycarbonyl]phenyl}ferrocene-1,1′-dicarboxylate (4a). Ferrocene-1,1′-dicarbonyl dichloride (0.4 g, 1.3 mmol) and triethylamine (2 ml) in 30 ml of methylene chloride were added to compound **3a** (1.6 g, 2.3 mmol) in 10 ml of methylene chloride. The reaction mixture was refluxed for 8 h, and the solvent was removed by evaporation under reduced pressure, and the crude product was purified by column chromatography (silica gel, 40–60 μm, using methylene chloride as the eluent) to yield 1.38 g (yield: 71%) of an orange solid. ^{1}H-NMR ($CDCl_3$, TMS, δ, ppm): 0.87–0.90 (m, 18H, CH_3), 1.26–1.53 (m, 36H, CH_3(CH_2)$_3$), 1.72–1.87 (m, 12H, OCH_2CH_2), 4.05–4.07 (m, 12H, OCH_2), 4.67 (t, 4Cp, β(ferrocene) to CO_2, $J=1.9$ Hz), 5.13 (t, 4Cp, α(ferrocene) to CO_2, $J=1.9$ Hz), 7.28–7.31 (m, 8Ar-H, 2 *m* to O_2C), 7.39 (d, 4Ar-H, *o* to O_2C-Cp, $J=8.7$ Hz), 7.42 (s, 4Ar-H, tris(hexyloxy)phenyl), 7.61–7.64 (m, 8Ar-H, 2 *o* (biphenyl) to CO_2), 8.27 (d, 4Ar-H, *m* to OH, $J=8.7$ Hz); Anal. Calcd for $C_{98}H_{130}O_{10}Fe$: C, 72.18; H, 6.96. Found: C, 72.35; H, 6.92%.

Compounds **4b**–**4h** were prepared by a similar method to that described for compound **4a**.

Bis{4-[4′-(3″,4″,5″-tris(octyloxy)phenylcarbonyloxy)biphenyloxycarbonyl]phenyl}ferrocene-1,1′-dicarboxylate (4b). Yield: 70%; ^{1}H-NMR ($CDCl_3$, TMS, δ, ppm): 0.87–0.90 (m, 18H, CH_3), 1.26–1.55 (m, 60H, CH_3(CH_2)$_5$), 1.72–1.87 (m, 12H, OCH_2CH_2), 4.02–4.09 (m, 12H, OCH_2), 4.67 (t, 4Cp, β(ferrocene) to CO_2, $J=1.9$ Hz), 5.12 (t, 4Cp, α(ferrocene) to CO_2, $J=1.9$ Hz), 7.28–7.31 (m, 8Ar-H, 2 *m* to O_2C), 7.39 (d, 4Ar-H, *o* to O_2C-Cp, $J=8.7$ Hz), 7.42 (s, 4Ar-H, tris(octyloxy)phenyl), 7.61–7.65 (m, 8Ar-H, 2 *o* (biphenyl) to CO_2), 8.27 (d, 4Ar-H, *m* to OH, $J=8.7$ Hz); Anal. Calcd for $C_{110}H_{146}O_{10}Fe$: C, 73.58; H, 7.61. Found C, 73.54; H, 7.61%.

Bis{4-[4′-(3″,4″,5″-tris(decyloxy)phenylcarbonyloxy)biphenyloxycarbonyl]phenyl}ferrocene-1,1′-dicarboxylate (4c). Yield: 75%; ^{1}H-NMR ($CDCl_3$, TMS, δ, ppm): 0.85–0.90 (m, 18H, CH_3), 1.26–1.55 (m, 84H, CH_3(CH_2)$_7$), 1.74–1.86 (m, 12H, OCH_2CH_2), 4.02–4.09 (m, 12H, OCH_2), 4.68 (t, 4Cp, β(ferrocene) to CO_2, $J=1.9$ Hz), 5.11 (t, 4Cp, α(ferrocene) to CO_2, $J=1.9$ Hz), 7.28–7.31 (m, 8Ar-H, 2 *m* to O_2C), 7.39 (d, 4Ar-H, *o* to O_2C-Cp, $J=8.7$ Hz), 7.42 (s, 4Ar-H, tris(decyloxy)phenyl), 7.61–7.67 (m, 8Ar-H, 2 *o* (biphenyl) to CO_2), 8.27 (d, 4Ar-H, *m* to OH, $J=8.6$ Hz); Anal. Calcd for $C_{122}H_{170}O_{10}Fe$: C, 74.59; H, 8.17. Found C, 74.47; H, 8.54%.

Bis{4-[4′-(3″,4″,5″-tris(dodecyloxy)phenylcarbonyloxy)biphenyloxycarbonyl]phenyl}ferrocene-1,1′-dicarboxylate (4d). Yield: 68%; ^{1}H-NMR ($CDCl_3$, TMS, δ, ppm): 0.85–0.90 (m, 18H, CH_3), 1.26–1.50 (m, 108H, CH_3(CH_2)$_9$), 1.74–1.86 (m, 12H, OCH_2CH_2), 4.02–4.09 (m, 12H, OCH_2), 4.68 (t, 4Cp, β(ferrocene) to CO_2, $J=1.9$), 5.13 (t, 4Cp, α(ferrocene) to CO_2, $J=1.9$ Hz), 7.28–7.31 (m, 8Ar-H, 2 *m* to O_2C), 7.35 (d, 4Ar-H, *o* to O_2C-Cp, $J=8.7$ Hz), 7.39 (s, 4Ar-H, tris(dodecyloxy)phenyl), 7.61–7.68 (m, 8Ar-H, 2 *o* (biphenyl) to CO_2), 8.27 (d, 4Ar-H, *m* to OH, $J=8.7$ Hz); Anal. Calcd for $C_{134}H_{194}O_{10}Fe$: C, 75.45; H, 8.66. Found: C, 75.49; H, 9.10%.

Bis{4-[4′-(3″,4″,5″-tris(tetradecyloxy)phenylcarbonyloxy)biphenyloxycarbonyl]phenyl}ferrocene-1,1′-dicarboxylate (4e). Yield: 72%; ^{1}H-NMR ($CDCl_3$, TMS, δ, ppm): 0.85–0.90 (m, 18H, CH_3), 1.18–1.49 (m, 132H, CH_3(CH_2)$_{11}$), 1.71–1.86 (m, 12H, OCH_2CH_2), 4.02–4.09 (m, 12H, OCH_2), 4.69 (t, 4Cp, β(ferrocene) to CO_2, $J=1.9$ Hz), 5.13 (t, 4Cp, α(ferrocene) to CO_2, $J=1.9$ Hz), 7.27–7.34 (m, 8Ar-H, 2 *m* to O_2C), 7.39 (d, 4Ar-H, *o* to O_2C-Cp, $J=8.7$ Hz), 7.42 (s, 4Ar-H, tris(tetradecyloxy)phenyl), 7.62–7.68 (m, 8Ar-H, 2 *o* (biphenyl) to CO_2), 8.27 (d, 4Ar-H, *m* to OH, $J=8.7$ Hz); Anal. Calcd for $C_{146}H_{218}O_{10}Fe$: C, 76.18; H, 9.07. Found C, 76.15; H, 9.15%.

Bis{4-[4′-(3″,4″,5″-tris(hexadecyloxy)phenylcarbonyloxy)biphenyloxycarbonyl]phenyl}ferrocene-1,1′-dicarboxylate (4f). Yield: 60%; ^{1}H-NMR ($CDCl_3$, TMS, δ, ppm): 0.85–0.90 (m, 18H, CH_3), 1.18–1.49 (m, 156H, CH_3(CH_2)$_{13}$), 1.74–1.86 (m, 12H, OCH_2CH_2), 4.02–4.06 (m, 12H, OCH_2), 4.69 (t, 4Cp, β(ferrocene) to CO_2, $J=1.9$ Hz), 5.13 (t, 4Cp, α(ferrocene) to CO_2, $J=1.9$ Hz), 7.27–7.34 (m, 8Ar-H, 2 *m* to O_2C), 7.39 (d, 4Ar-H, *o* to O_2C-Cp, $J=8.7$ Hz), 7.42 (s, 4Ar-H, tris(hexadecyloxy)phenyl), 7.62–7.68 (m, 8Ar-H, 2 *o* (biphenyl) to CO_2), 8.27 (d, 4Ar-H, *m* to OH, $J=8.7$ Hz); Anal. Calcd for $C_{158}H_{242}O_{10}Fe$: C, 76.82; H, 9.42. Found C, 76.79; H, 9.56%.

Bis{4-[4′-(3″,4″,5″-tris(octadecyloxy)phenylcarbonyloxy)biphenyloxycarbonyl]phenyl}ferrocene-1,1′-dicarboxylate (4g). Yield: 73%; ^{1}H-NMR ($CDCl_3$, TMS, δ, ppm): 0.85–0.90 (m, 18H, CH_3), 1.18–1.49 (m, 180H, CH_3(CH_2)$_{15}$), 1.74–1.86 (m, 12H, OCH_2CH_2), 4.02–4.09 (m, 12H, OCH_2), 4.69 (t, 4Cp, β(ferrocene) to CO_2, $J=1.9$ Hz), 5.13 (t, 4Cp, α(ferrocene) to CO_2, $J=1.9$ Hz), 7.28–7.34 (m, 8Ar-H, 2 *m* to O_2C), 7.39 (d, 4Ar-H, *o* to O_2C-Cp, $J=8.7$ Hz), 7.42 (s, 4Ar-H, tris(octadecyloxy)phenyl), 7.61–7.65 (m, 8Ar-H, 2 *o* (biphenyl) to CO_2), 8.27 (d, 4Ar-H, *m* to OH, $J=8.7$ Hz); Anal. Calcd for $C_{170}H_{266}O_{10}Fe$: C, 77.37; H, 9.74. Found C, 77.34; H, 9.72%.

Bis{4-[4′-(3″,4″,5″-tris(eicosyloxy)phenylcarbonyloxy)biphenyloxycarbonyl]phenyl}ferrocene-1,1′-dicarboxylate (4h). Yield: 66%; ^{1}H-NMR ($CDCl_3$, TMS, δ, ppm): 0.85–0.90 (m, 18H, CH_3), 1.18–1.49 (m, 204H, CH_3(CH_2)$_{17}$), 1.74–1.86 (m, 12H, OCH_2CH_2), 4.02–4.09 (m, 12H, OCH_2), 4.69 (t, 4Cp,

β(ferrocene) to CO_2, $J=1.9$ Hz), 5.13 (t, 4Cp, α(ferrocene) to CO_2, $J=1.9$ Hz), 7.28–7.34 (m, 8Ar-H, 2 *m* to O_2C), 7.39 (d, 4Ar-H, *o* to O_2C-Cp, $J=8.7$ Hz), 7.42 (s, 4Ar-H, tris(eicosyloxy)-phenyl), 7.61–7.65 (m, 8Ar-H, 2 *o* (biphenyl) to CO_2), 8.27 (d, 4Ar-H, *m* to OH, $J=8.7$ Hz); Anal. Calcd for $C_{182}H_{290}O_{10}Fe$: C, 77.86; H, 10.01. Found C, 77.79; H, 10.18%.

Results and discussion

Synthesis and thermal characterization

The synthesis of ferrocene containing hexacatenar metallomesogens was performed according to the procedure described in Scheme 1. The metallomesogenic precursor molecules **3a–h** were synthesized by esterification of 3,4,5-trialkoxy substituted benzoic acid with biphenyldiol and another esterification with 4-benzyloxybenzoic acid. The resulting precursors **3a–h** were treated with ferrocene-1,1′-dicarbonyl dichloride to yield ferrocene containing hexacatenar metallomesogens **4a–h** based on alkoxy terminal groups from hexyloxy to dodecyloxy. All analytical data of the metallomesogenic molecules are consistent with expected structures.

The thermotropic phase behavior of the ferrocene containing metallomesogens was investigated by a combination of techniques consisting of differential scanning calorimetry (DSC), thermal optical polarized microscopy and X-ray scattering experiments. Fig. 1 presents the DSC heating and cooling curves of the metallomesogens. The transition temperatures and the corresponding enthalpy changes of all complexes obtained from DSC are summarized in Table 1. In contrast to the precursor molecules which exhibit only a crystalline phase, all the metallomesogens except **4a** and **4h** exhibit a thermotropic liquid crystalline phase. As can be observed from Fig. 1 and Table 1, **4a** based on hexyloxy terminal chains exhibits only a crystalline melting at 200.2 °C. In contrast, **4b** based on octyloxy terminal chains shows a crystalline melting at 162.9 °C, followed by a mesophase which, in turn, undergoes transformation into an isotropic liquid at 172.9 °C. **4c** shows a similar phase behavior to that of **4b** which exhibits a crystalline melting followed by a mesophase. On optical microscopy, however, no birefringence between cross polarizers after melting of **4b** and **4c** could be observed, strongly suggesting the existence of an optically isotropic cubic mesophase.[16]

The metallomesogen **4d** based on dodecyloxy terminal chains exhibits a crystalline melting at 117.1 °C, followed by a mesophase which, in turn, undergoes transformation into isotropic liquid at 172.3 °C. Optical microscopic observations of this compound are consistent with this behavior. Transition from an isotropic liquid can be seen by the formation of dendritic domains which merge into a pseudo-focal conic texture which is characteristic of a hexagonal columnar mesophase exhibited by other hexagonal columnar liquid crystals.[17,18] The ferrocene complexes **4e**, **4f** and **4g** also show phase behavior similar to that of the complex **4d** which exhibits a crystalline melting followed by a hexagonal columnar mesophase. Fig. 2 shows a representative texture exhibited by the hexagonal columnar liquid crystalline phase of **4d**. Further increasing the length of flexible coil as in the case of **4h** suppresses the formation of liquid crystallinity. This is most probably due to the high entropic contribution of the long terminal chains on the melt state.

The thermal behavior of the metallomesogens based on ferrocene determined from heating and cooling DSC curves as well as thermal optical polarized microscopy is presented in Fig. 3. As shown in Fig. 3, the transition temperatures associated with the crystalline melting decrease and the mesophase temperature ranges become broader with increasing length of terminal chains. A notable feature in this figure is the existence of a cubic phase in the compounds containing short terminal carbon chains. Similar to lyotropic and conventional

Table 1 Thermal transitions of the ferrocene containing hexacatenar metallomesogens[a]

Compound	Phase transition/°C (corresponding enthalpy changes/kJ mol^{-1})[a]	
	Heating	Cooling
4a	k 200.2 (69.8) i	i 159.6 (78.6) k
4b	k 162.9 (69.4) bcc 172.9 (7.2) i	i 158.0 (2.2) bcc 143.8 (67.0) k
4c	k 126.5 (128.7) bcc 174.6 (4.4) i	i 162.2 (3.2) bcc
4d	k 117.1 (98.9) col 172.3 (1.6) i	i 165.1 (1.4) col
4e	k 112.6 (82.9) col 170.7 (1.8) i	i 164.7 (1.7) col
4f	k 120.4 (110.0) col 171.9 (1.4) i	i 169.0 (2.1) col 62.7 (69.0) k
4g	k 120.9 (120.4) col 172.9 (1.6) i	i 169.5 (2.0) col 92.8 (122.8) k
4h	k 118.5 (122.0) i	i 97.0 (135.5) k 58.7 (34.2) k

[a]k = crystalline, bcc = bicontinuous cubic, col = hexagonal columnar, i = isotropic.

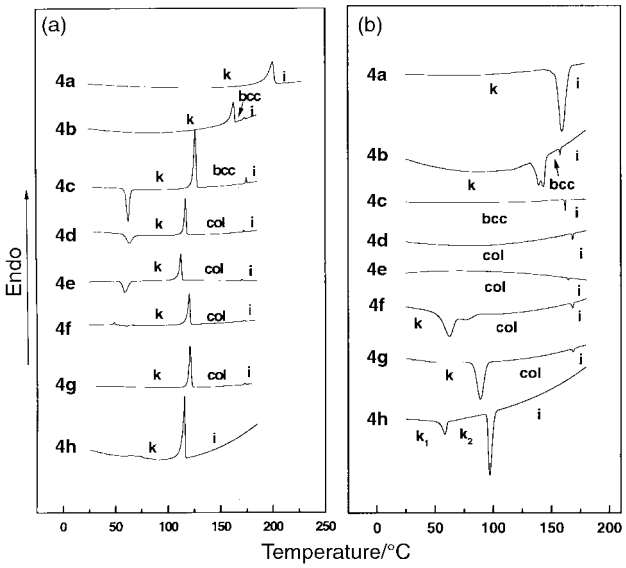

Fig. 1 DSC diagram exhibited during (a) the second heating scan and (b) the first cooling scan by ferrocene containing hexacatenar metallomesogens.

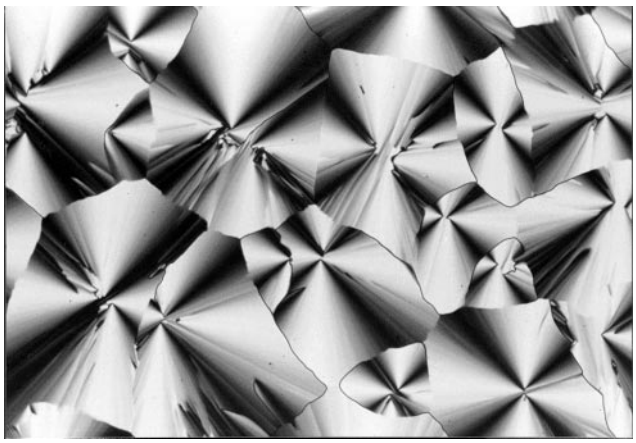

Fig. 2 Representative optical micrography (100 ×) of texture exhibited by the hexagonal columnar mesophase of **4f** at 168 °C on a cooling scan.

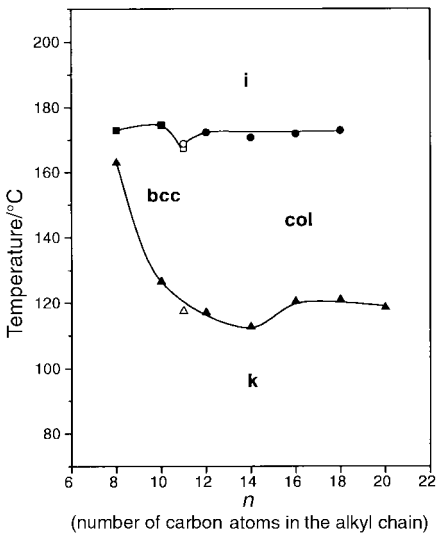

Fig. 3 Dependence of the phase-transition temperature of **4a**–**h**. Data are obtained from the DSC heating scan. The open symbols for $n=11$ are obtained from the equimolar mixture of **4c** and **4d** (k, crystalline; bcc, bicontinuous cubic; col, columnar; i, isotropic).

block copolymer systems,[19,20] the topology in this region should be a bicontinuous cubic phase since such a structure can attain a smaller interfacial curvature than those of the columnar phase. Therefore, we assume that the complexes based on octyloxy and decyloxy terminal chains exhibit a bicontinuous cubic phase. Interestingly, the equimolar mixture of **4c** and **4d** exhibits both a cubic phase at lower temperatures and a columnar phase at higher temperatures.

X-Ray diffraction studies

To investigate the self-assembled crystalline and liquid crystalline states, X-ray scattering experiments have been performed with the selected complexes at various temperatures. The first order spacings and the lattice constants determined by small angle X-ray diffractions are summarized in Table 2. In the crystalline state, the X-ray diffraction pattern of the complex **4a** displays three reflections in the spacing ratio of 1, 1/2, 1/3 in the small angle region, while a number of sharp reflections are observed in the wide angle region, indicative of a lamellar structure consisting of a microphase separated aromatic rod domains and the aliphatic chain domains with a lattice constant of 34.9 Å. The layer spacings are close to the corresponding estimated repeating unit length of the metallomesogenic molecules, indicative of a monolayer lamellar structure in which rod units are fully interdigitated.

The X-ray diffraction pattern of **4c** in its liquid crystalline state displays several sharp reflections in the small angle region as shown in Fig. 4. The relative positions of these reflections are $1/\sqrt{6}$, $1/\sqrt{8}$, $1/\sqrt{14}$, $1/\sqrt{16}$, $1/\sqrt{22}$, $1/\sqrt{24}$ which can be indexed as the 211, 220, 321, 400, 332 and 442 reflections of a body centered cubic phase with *Ia*3*d* symmetry.[12] From the observed *d*-spacing of the 211 reflection, the best fit value for the lattice

Table 2 Characterization of the ferrocence containing hexacatenar metallomesogens by small angle X-ray scattering

	Crystalline phase	Liquid crystalline phase			
		Cubic		Columnar	
	Lamellar				
Compound	d_{001}/Å	d_{211}/Å	Lattice constant *a*/Å	d_{100}/Å	Lattice constant *a*/Å
4a	34.9				
4c		55.8	136.7		
4d				55.7	64.3
4h	69.9				

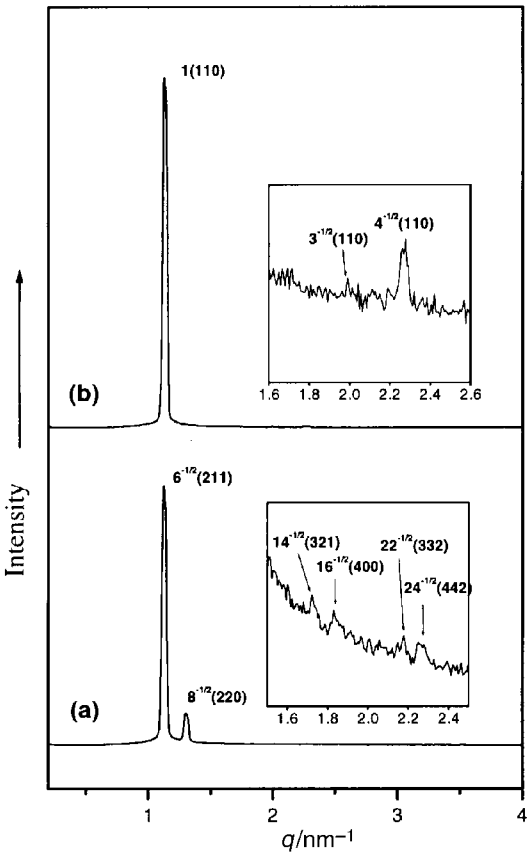

Fig. 4 SAXS spectra obtained in (a) the bicontinuous cubic mesophase at 150 °C for **4c** and (b) the hexagonal columnar mesophase at 150 °C for **4d** [$q=4\pi\sin(\theta/\lambda)$].

parameter for the cubic phase of **4c** is 136.7 Å. At a wide angle only a diffuse halo remains for all the rod–coil molecules as evidence of the lack of any positional long-range order other than the three dimensional cubic packing of supramolecular units (Fig. 5).

On the basis of the X-ray diffraction data described above and its position in the phase diagram, located between lamellar crystalline and hexagonal columnar liquid crystalline structures, the cubic phase can be best described as a bicontinuous cubic phase with *Ia*3*d* symmetry occurring frequently in lyotropic systems.[20] Thus a similar model proposed for the lyotropic bicontinuous cubic phase may be used for its description. Although a bicontinuous cubic phase with *Ia*3*d* symmetry is commonly observed in both lyotropic amphiphilic systems and conventional diblock copolymers, it has been observed in relatively few thermotropic systems such as amphiphilic glucitol derivatives,[21] polycatenar silver complexes,[22] and glycolipid derivatives.[23] In particular, formation of thermotropic bicontinuous cubic phases in ferrocene containing metallomesogenic systems is very rare.

The X-ray diffraction pattern of the birefringent mesophase of **4d** displays three sharp reflections with the ratio of $1:1/\sqrt{3}:1/\sqrt{4}$ in the small angle region, characteristic of the two-dimensional hexagonal structure (hexagonally packed supramolecular cylinders) with a lattice constant of 64.3 Å.[17] The observed *d*-spacings and the lattice constants are given in Table 2 and a representative small angle X-ray diffraction pattern of **4d** is shown in Fig. 4. At the wide angles only a diffuse halo remains as evidence of a lack of any positional long range order other than the two dimensional hexagonal packing of supramolecular columns (Fig. 5). These results together with optical microscopic observations indicate that this complex displays a disordered hexagonal columnar mesophase.

On the basis of the X-ray results, schematic representations can be constructed as shown in Fig. 6. A notable feature of our

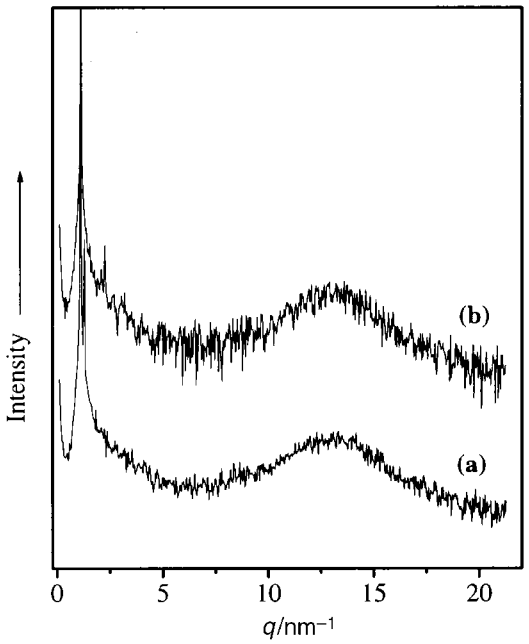

Fig. 5 WAXS patterns of (a) the **4c** and (b) the **4d** at a liquid crystalline phase [$q=4\pi\sin(\theta/\lambda)$].

system consists in the ability of the metallomesogens based on ferrocene building blocks to self-assemble into ordered structures with curved interfaces in their liquid crystalline states. Formation of bicontinuous cubic and hexagonal/columnar assemblies in the metallomesogens is in contrast to the general behavior of conventional liquid crystalline molecules based on rigid rod-like mesogens.[24] The molecular organization of the metallomesogens into the bicontinuous cubic or the columnar structures is also remarkably different from that usually observed in those of block polymers based on immiscible coil blocks since the ferrocene containing aromatic rod segments consisting of a core domain favor anisotropic aggregation with their long axes even in the melt state, rather than isotropic aggregation.

Formation of the ordered structures with interfacial curvature from the rod-like metallomesogens can be rationalized by considering the entropic penalties associated with the chain stretching and anisotropic arrangement of aromatic rod segments. Trisubstituted flexible alkoxy chains induce curvature at the aromatic/aliphatic interface, arising from the connectivity of the stiff rod and flexible chains, constraint of constant density, and minimization of chain stretching. At the interface separating the rod and chain domains in the layered structure, the relatively smaller area per junction favored by rod–block results in chain stretching of the aliphatic segments, which is energetically unfavorable. Therefore, the molecules self-assemble into bicontinuous cubic or hexagonal columnar

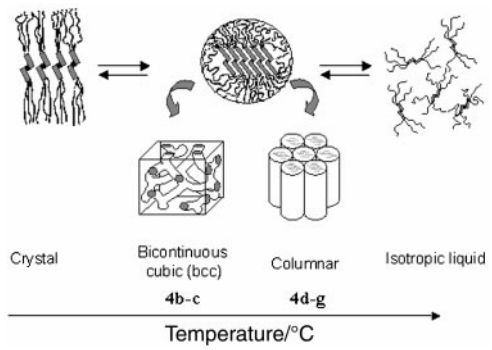

Fig. 6 Schematic representation of the self-assemblies of ferrocene containing hexacatenar metallomesogens.

structures with a larger interfacial area, instead of a layered smectic structure.

The results described in this paper demonstrate that systematic variation in the length of coil in the ferrocene containing metallomesogenic system can change the supramolecular architecture from lamellar, bicontinuous cubic to hexagonal columnar phases. The main organizing forces responsible for this change are believed to be the anisotropic orientation of ferrocene containing rod segments and consequent entropic penalties associated with chain stretching.

Conclusion

We have prepared hexacatenar metallomesogens based on ferrocene. The resulting metallomesogens were characterized by DSC, thermal optical microscopy and X-ray scattering measurements. In the crystalline state, the metallomesogens have been observed to organize into a microphase separated monolayer lamellar structure. In the liquid crystalline state, the metallomesogens with octyloxy and decyloxy terminal groups **4b** and **4c** self-assemble into an optically isotropic cubic mesophase. This phase has been identified by X-ray scattering methods to be a bicontinuous cubic phase with *Ia3d* symmetry. Increasing the length of the terminal chains induces a hexagonal columnar mesophase as exhibited by **4d**, **4e**, **4f** and **4g**. Further increasing the length of the terminal chains as in the case of **4h** suppresses liquid crystallinity and gives rise to only a crystalline phase. This unique phase behavior in the ferrocene containing metallomesogens can be understood to originate from the anisotropic aggregation of rod segments and consequent entropic penalties associated with chain stretching. These results demonstrate that a rich variety of self-assembled supramolecular structures can be induced in the rod-like metallomesogenic systems through the introduction of different lengths of terminal chains.

Acknowledgements

This work was supported by the Korea Science and Engineering Foundation (2000) and CRM-KOSEF (2000).

References

1 M. Muthukumar, C. K. Ober and E. L. Thomas, *Science*, 1997, **277**, 1225.
2 J. M. J. Frechet, *Science*, 1994, **263**, 1710.
3 S. A. Jenekhe and X. L. Chen, *Science*, 1998, **279**, 1903.
4 J. L. Serrano, *Metallomesogens*, ed. J. L. Serrano, VCH, Weinheim, Germany, 1995.
5 B. Donnio, J. M. Seddon and R. Deschenaux, *Organometallics*, 2000, **19**, 3077.
6 R. Deschenaux, M. Schweissguth, M.-T. Vilches, A.-M. Levelut, D. Hautot and D. Luneau, *Organometallics*, 1999, **18**, 5553.
7 B. Dardel, R. Deschenaux, M. Even and E. Serrano, *Macromolecules*, 1999, **32**, 5193.
8 H. J. Coles, S. Meyer, P. Lehmann, R. Deschenaux and I. Jausline, *J. Mater. Chem.*, 1999, **9**, 1085.
9 R. Deschenaux and J. L. Marendaz, *J. Chem. Soc., Chem. Commun.*, 1991, 909.
10 R. Deschenaux, I. Kosztics and B. Nicolet, *J. Mater. Chem.*, 1995, **5**, 2291.
11 R. Deschenaux, M. Rama and J. Santiago, *Tetrahedron Lett.*, 1993, **34**, 3293.
12 J. Andersch, S. Diele and C. Tschierske, *J. Mater. Chem.*, 1996, **6**, 1465.
13 R. Deschenaux, E. Serrano and A.-M. Levelut, *Chem. Commun.*, 1997, 1577.
14 G. Kenneth, Z. Lin and D. R. Marvin, *J. Am. Chem. Soc.*, 1984, **106**, 3862.
15 M. Lee, Y.-S. Yoo and M.-G. Choi, *Bull. Korean Chem. Soc.*, 1997, **18**, 1067.
16 D. Demus and L. Richter, *Textures of Liquid Crystals*, Verlag Chemie, Weinheim, Germany, 1978; G. W. Gray and

J. W. Goodby, *Smectic Liquid Crystals. Textures and Structures*, Leonard Hill, Glasgow, UK, 1985.
17 M. Lee, B.-K. Cho, H. Kim, J.-Y. Yoon and W.-C. Zin, *J. Am. Chem. Soc.*, 1998, **120**, 9168.
18 C. Destrade, P. Foucher, H. Gasparoux and H. T. Nguyen, *Mol. Cryst. Liq. Cryst.*, 1984, **106**, 121.
19 S. Forster, A. K. Khandpur, J. Zhao, F. S. Bates, I. W. Hamley, A. J. Ryan and W. Bras, *Macromolecules*, 1994, **27**, 6922.
20 Y. Rancon and J. Charvolin, *J. Phys. Chem.*, 1988, **92**, 2646.
21 K. Borisch, S. Diele, P. Goering, H. Mueller and C. Tschierske, *Liq. Cryst.*, 1997, **22**, 427.
22 B. Donnio, B. Heinrich, T. Gulik-Krzywicki, H. Delacroix, D. Guillon and D. W. Bruce, *Chem. Mater.*, 1997, **9**, 2951; B. Donnio, D. W. Bruce, H. Delacroix and T. Gulik-Krzywicki, *Liq. Cryst.*, 1997, **23**, 147.
23 S. Fishcer, H. Fischer, S. Diele, G. Pelzl, K. Jankowski, R. R. Schmidt and V. Vill, *Liq. Cryst.*, 1994, **17**, 855.
24 H. Stegemeyer, guest ed., 'Liquid Crystals', *Top. Phys. Chem.*, 1994, 3.